Korean J. Chem. Eng., **21**(1), 59-68 (2004)

Flow Direction When Fan Shaped Geometry is Applied in Gas-Assisted Injection Molding: 2. Development of Flow Model and its Predictions

Kwang-Hee Lim† and Soo Hyeun Hong

Department of Chemical Engineering, Daegu University, Kyungsan, Kyungbook 712-714, Korea
(*Received 3 April 2003 • accepted 30 December 2003*)

Abstract−In part 2 of the paper simplified unsteady-mass (and momentum-) balance equations of melt polymer resin in the cavities of GAIM were proposed, as a time-dependent rule of thumb, to constitute a novel flow model in GAIM under the configuration of two fan-shaped geometries connected with a gas nozzle. Upon performing a simulation on them with commercial software (MOLDFLOW), we compared the time evolution of simulated gas penetration lengths with the those of unsteady trajectory on the gas flow in GAIM by the suggested novel flow model in the fan-shaped cavities in order to check the precision of model-predicted gas penetration lengths as well as the consistency of its predicted direction. The results by the suggested novel flow model were satisfactory to fit the trajectory simulated with commercial software (MOLDFLOW).

Key words: Gas-Assisted Injection Molding, Rule of Thumb, Preferred Direction of Gas, Novel Flow Model, Trajectory of Gas Flow, Gas Penetration

INTRODUCTION

Most gas-assisted injection molded parts are, by and large, composed not only of a single section through which gas penetrates but also a nominal thin wall with gas channels traversing the parts. To design molds in such a way that the gas cores out all the channels or other thick sections without penetrating into the thin walls, one needs to predict the preferred direction of gas for a given geometry. The understanding of rules governing the preferred direction of gas is important for trouble shooting during mold try outs as well as in design stage. Many researchers [Chen, 1995; Khayat et al., 1995; Chen et al., 1996a, b; Gao et al., 1997; Shen, 1997, 2001; Parvez et al., 2002] have investigated primary and secondary gas penetration in terms of gas-liquid interface and polymer melt front in GAIM. However, their approaches cannot be regarded as a rule of thumb but are close to the commercial software for GAIM in that numerical simulations are performed by the use of control volume/finite element method or boundary-element approach. The rule of thumb on the direction of gas flow for GAIM has been investigated [Lim and Soh, 1999; Soh and Lim, 2002; Lim and Lee, 2003; Lim, 2003] and simulation packages were used to verify the gas direction predicted by the rule of thumb. Lim and Soh [1999] assumed that pressure difference between a gas injection point and appropriate vent areas at both sides of well-maintained molds are equal. Consequently, the pressure drops at both sides are equated to compare the resistances and to predict the gas direction. Soh and Lim [2002] suggested a definition of the resistance to velocity to predict the gas-preferred direction under the simplest geometry of two different pipes connected at one connection point. In such a complex situation as runners or thick cavity of two square plates connected to cavities composed of four pipes with same length and different diameter connected in series and parallel, Lim and Lee [2003] proposed a criterion in the prediction of gas flow direction of GAIM as the resistance to the initial velocity of melt polymer at the nearest geometry to a gas injection point and showed why a comparison of the resistances to flow rates of resin often leads to a wrong prediction for the gas direction, while the comparison of proposed resistances generally leads to a valid prediction of gas-preferred direction.

In part 1 of this paper [Lim, 2003] the qualitative analytical method (a rule of thumb) to predict the preferred gas flow direction in gas-assisted injection molding (GAIM) process, which involves the flow through panel-areas of various fan-shaped geometries, and the criteria to apply the method were presented with appropriate assumptions. The predictions with the suggested rule of thumb were quite well matched by the simulation-results of MOLDFLOW (version of MPI 4.0). However, the discrepancy between the ratio of distances traveled and the ratio of resistances was observed to increase as the ratio of the values of H/R_0 on the right and left hand side of fan-shaped cavities became greater, even though the suggested rule of thumb was assumed adequate to use until the case met the condition of $(H/R_0)^2(1/\hat{\theta}^2)<<1$ and $(H/R_0)^2<<1$, which calls for a time-dependent rule of thumb that is a model-based trajectory analysis of the interface of gas and melt resin compared to the simulation results by commercial software to understand time-dependent behavior of gas and melt front in GAIM. Nevertheless, the suggested rule of thumb was still effective as far as the direction of gas flow was concerned.

According to the necessity of developing a time-dependent rule of thumb, in part 2 of the paper, we propose simplified unsteady-mass (and momentum-) balance equations of melt polymer resin in cavities of GAIM to constitute a novel flow model in GAIM under the configuration of two fan-shaped geometries connected with a gas nozzle or a needle. Upon performing the simulation on them with commercial software (MOLDFLOW) we compare the simulated gas penetration lengths with the those of unsteady trajectory on the gas flow in GAIM by the suggested novel unsteady mass (and momentum-) balance equations of melt polymer resin in the

†To whom correspondence should be addressed.
E-mail: khlim@daegu.ac.kr

fan-shaped cavities in order to check the precision of the predicted gas penetration lengths by the novel flow model as well as the consistency of its predicted direction.

METHODS

1. Theory

1-1. Flow Model Under Fan-shaped Geometry Neglecting Coated Layer on the Surface of Molds

In part 1 of this paper [Lim, 2003] the expression of the flow rate of melt phase (Q) was obtained from the flow model neglecting frozen layers on the surface of cavity of molds for the fan-shaped geometry.

$$Q=\hat{\theta}rH\langle v_r\rangle=2\int_0^h v_r(r,z)\hat{\theta}r\,dz=\frac{2}{3}\frac{\hat{\theta}h^3}{\mu}\frac{P_1-P_0}{\ln\frac{R_0}{R_1}} \tag{1}$$

where $\langle v_r\rangle$ is average velocity of melt phase flow.

Thus, the pressure drop between R_1 and R_0 may be written in terms of flow rate as below.

$$\Delta P=\frac{12\mu Q}{H^3\hat{\theta}}\ln\frac{R_0}{R_1}=Q\frac{12\mu}{H^3\hat{\theta}}\ln\frac{R_0}{R_1} \tag{2}$$

Using the relation of $Q=R_1\hat{\theta}HV_1$, the flow rate may be expressed in such a way as:

$$Q=\frac{\hat{\theta}}{2}H\frac{dR_1^2}{dt} \tag{3}$$

One may substitute Eq. (3) into Eq. (2) and separate variables in both sides, after which both sides are integrated to develop the flow model to show dynamics of R_1 and R_0 as below.

$$\therefore\int_0^t\Delta P\,dt=\frac{6\mu}{H^2}\int_{R_1^2(0)}^{R_1^2}\ln\frac{R_0}{R_1}dR_1^2 \tag{4}$$

R_0 (0) and R_1 (0) are resin length at polymer shut-off and the radius of gas nozzle, respectively.

The volume of melt polymer in fan-shaped geometry may be calculated and its value may be designated as A. Then the ratio of R_0 and R_1 may be obtained as below.

$$\left(\frac{R_0}{R_1}\right)^2=\frac{1}{R_1^2}\frac{2A}{\hat{\theta}H}+1 \tag{5}$$

where $\frac{2A}{\hat{\theta}H}=(R_0^2(0)-R_1^2(0))$

Substituting Eq. (5) into Eq. (4) with appropriate transformation, one may get the expression as:

$$\Delta Pt=\frac{3\mu}{H^2}\int_{X(0)}^{X}\ln\left(\frac{2A}{\hat{\theta}H}\frac{1}{X}+1\right)dX \tag{6}$$

where $X=R_1^2(t)$

After Eq. (6) is partially integrated one may obtain the equation that explains the dynamics of R_0 and R_1 as:

$$\Delta Pt=\frac{3\mu}{H^2}\left\{\left[R_1^2(t)\ln\left(\frac{2A}{\hat{\theta}H}\frac{1}{R_1^2(t)}+1\right)-R_1^2(0)\ln\left(\frac{2A}{\hat{\theta}H}\frac{1}{R_1^2(0)}+1\right)\right]\right.$$

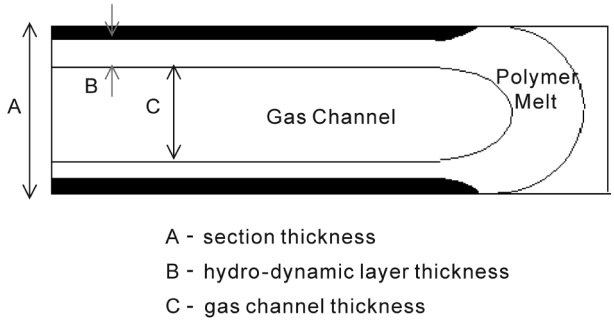

Fig. 1. Gas penetration in a freezing viscous fluid.

$$\left.+\left(\frac{2A}{\hat{\theta}H}\right)\ln\left(\frac{R_1(t)^2+\frac{2A}{\hat{\theta}H}}{R_1^2(0)+\frac{2A}{\hat{\theta}H}}\right)\right\} \tag{7}$$

where $\frac{2A}{\hat{\theta}H}=(R_0^2(0)-R_1^2(0))$

1-2. Flow Model Under Fan-shaped Geometry in Consideration of Coated Layer on the Surface of Molds

The relationship between the capillary number and the volume swept forward had been determined about the penetration of gas into Newtonian or Non-Newtonian fluids [Kolb and Cerro, 1991; Poslinski et al., 1995; Huzyak and Koelling, 1997; Gauri and Koelling, 1999]. Fig. 1 is a representation of gas penetration into a freezing viscous fluid. For a given section thickness (A), the thickness of the hydrodynamic layer (B) is dependent on the capillary number (Ca), a function of melt viscosity, surface tension and linear velocity of melt polymer. As the capillary number increases less material is pushed forward; in other words, the percentage of the melt resin that is left behind increases until it asymptotically approaches a certain value. At a typical working range of GAIM whose capillary number would be above 1,000, the gas will leave behind a certain value of fractions of the melt resin as hydrodynamic layer. In addition to hydrodynamic layer the frozen layer at the surface of molds should be also considered to determine the amount of coated layer left behind in GAIM.

One may consider coated layer (i.e., frozen layer and hydrodynamic layer) left behind when gas pushes the resin to flow forward as in Fig. 1. Since gas channel thickness becomes narrower, due to the existence of coated layer with thickness δ for one fan-shaped flat plate, than melt front thickness of resin pushed forward, the effective thickness of moving resin is assumed to be a value less by 2δ than the thickness between two plates of a cavity. When mass conservation is applied and volume contraction due to compression is ignored under the geometry as shown in Fig. 2(a)-(c), a new balance equation may be obtained:

$$\left(\frac{R_0}{R_1}\right)^2=\frac{1}{R_1^2}\left(\frac{2A}{\hat{\theta}H}+R_1^2(0)\frac{2\delta}{H}\right)+1-\frac{2\delta}{H} \tag{8}$$

where $\frac{2A}{\hat{\theta}H}=(R_0^2(0)-R_1^2(0))$ and δ=thickness of coated layer on one side of mold

Substituting H-2δ and Eq. (8) into Eq. (4) for H and $(R_0/R_1)^2$, re-

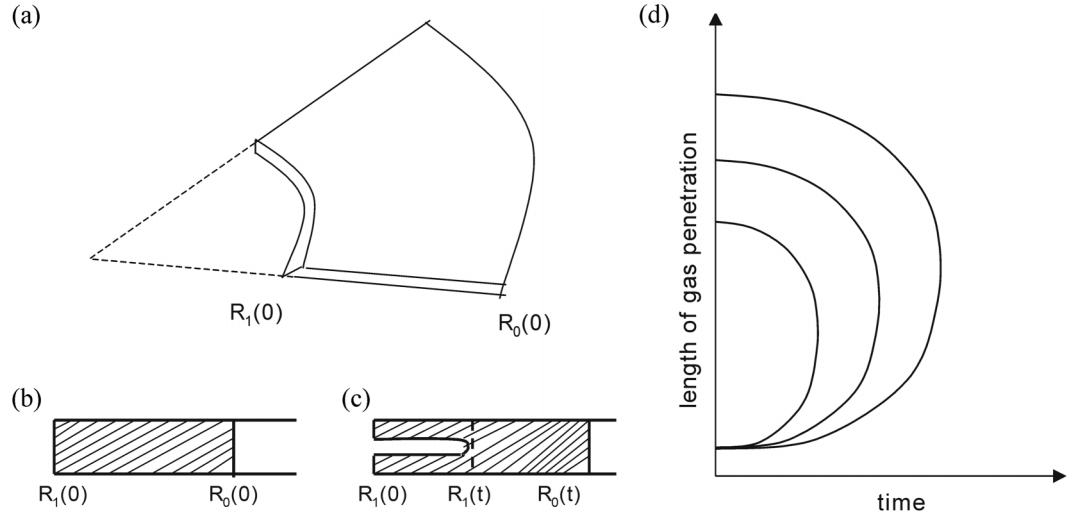

Fig. 2. Fan-shaped cavity of the mold: (a) Before melt-polymer is filled in the mold; (b) After melt-polymer is filled as short shot molding; (c) When gas is injected into the cavity filled by resin and the length of gas penetration increases; (d) Typical behavior of the solution of suggested flow model describing the length of gas penetration.

spectively, with appropriate transformation, one may get the expression as:

$$\Delta Pt = = \frac{3\mu}{(H-2\delta)^2}\int_{X(0)}^{X} \ln\left(\left(\frac{2A}{\tilde{\theta}H}+R_1^2(0)\frac{2\delta}{H}\right)\frac{1}{X}+\left(1-\frac{2\delta}{H}\right)\right)dX \quad (9)$$

where $X=R_1^2(t)$

After Eq. (9) is partially integrated one may obtain the equation that explains the dynamics of R_0 and R_1 as:

$$\begin{aligned}\Delta Pt = &\frac{3\mu}{(H-2\delta)^2}\Bigg[R_1^2(t)\ln\left(\left(\frac{2A}{\tilde{\theta}H}+R_1^2(0)\frac{2\delta}{H}\right)\frac{1}{R_1^2(t)}+\left(1-\frac{2\delta}{H}\right)\right)\\ &-R_1^2(0)\ln\left(\left(\frac{2A}{\tilde{\theta}H}+R_1^2(0)\frac{2\delta}{H}\right)\frac{1}{R_1^2(0)}+\left(1-\frac{2\delta}{H}\right)\right)\\ &+\frac{3\mu}{(H-2\delta)^2}\left(\frac{\frac{2A}{\tilde{\theta}H}+R_1^2(0)\frac{2\delta}{H}}{1-\frac{2\delta}{H}}\right)\\ &\ln\left(\frac{\left(1-\frac{2\delta}{H}\right)R_1^2(t)+\frac{2A}{\tilde{\theta}H}+R_1^2(0)\frac{2\delta}{H}}{\left(1-\frac{2\delta}{H}\right)R_1^2(0)+\frac{2A}{\tilde{\theta}H}+R_1^2(0)\frac{2\delta}{H}}\right)\end{aligned} \quad (10)$$

where $\frac{2A}{\tilde{\theta}H}=(R_0^2(0)-R_1^2(0))$

2. Simulations and Model-predictions When Two Cavities of Fan-shaped Plates are Involved in Configuration

As in part 1 of the paper, two fan-shaped flows with a common gas-pressure were considered where lengths of polymer-shut off at both fans were adjusted to be the same in order to measure the effect of the process conditions other than initial resin length and to compare the dynamic behavior at both fans. In addition, two fan-shaped flows of a common gas-pressure and of the same angle of fans were simulated with different lengths of initial polymer shut-off as well as the different thickness of cavities to both left and right directions. The simulation conditions as well as geometrical conditions in each case are given as in Tables 1, 2, 4 and 6.

Table 1. Simulation conditions of MOLDFLOW

Simulation ractor	Description
Resin filling	Short shot molding (85-95%)
Gas control	Volume control
Resin	PET(DP400)
Resin melt temperature	210 °C
Mold temperature	100 °C
Gas injection pressure	15 M pascal
Gas delay time	0.5 sec
Gas piston time	1 sec

Table 2. Various geometrical conditions of fan-shaped cavities (1)

Case	Position	Vertex angle	Thickness	R_1	R_0
Fig. 3-1	Left	(a) 30°, (b) 60°, (c) 90°	2 mm	9.4 mm	43 mm
	Right	(a) 90°, (b) 90°, (c) 90°	3 mm	9.4 mm	43 mm
Fig. 3-2	Left	(a) 30°, (b) 60°	3 mm	9.4 mm	43 mm
	Right	(a) 90°, (b) 90°	2 mm	9.4 mm	43 mm
Fig. 3-3(a)	Left	30°	2 mm	9.4 mm	43 mm
	Right	90°	3 mm	9.4 mm	43 mm
Fig. 3-3(b)	Left	30°	2 mm	9.4 mm	43 mm
	Right	90°	4 mm	9.4 mm	43 mm
Fig. 3-3(c)	Left	30°	2 mm	9.4 mm	43 mm
	Right	90°	5 mm	9.4 mm	43 mm

• Fig. 3-1(a) is the same as Fig. 3-3(a).

After simulations were performed under various geometrical conditions, the model predictions on gas flow were performed in consideration of coated layer. In model-predictions, the coated layer thickness (δ) of one fan-shaped flat plate was assumed to be 20% of the thickness between two fan-shaped flat plates of molds in case of the model prediction of fan-shaped flow according to the simulation results showing that polymer fraction was ca. 40%, respec-

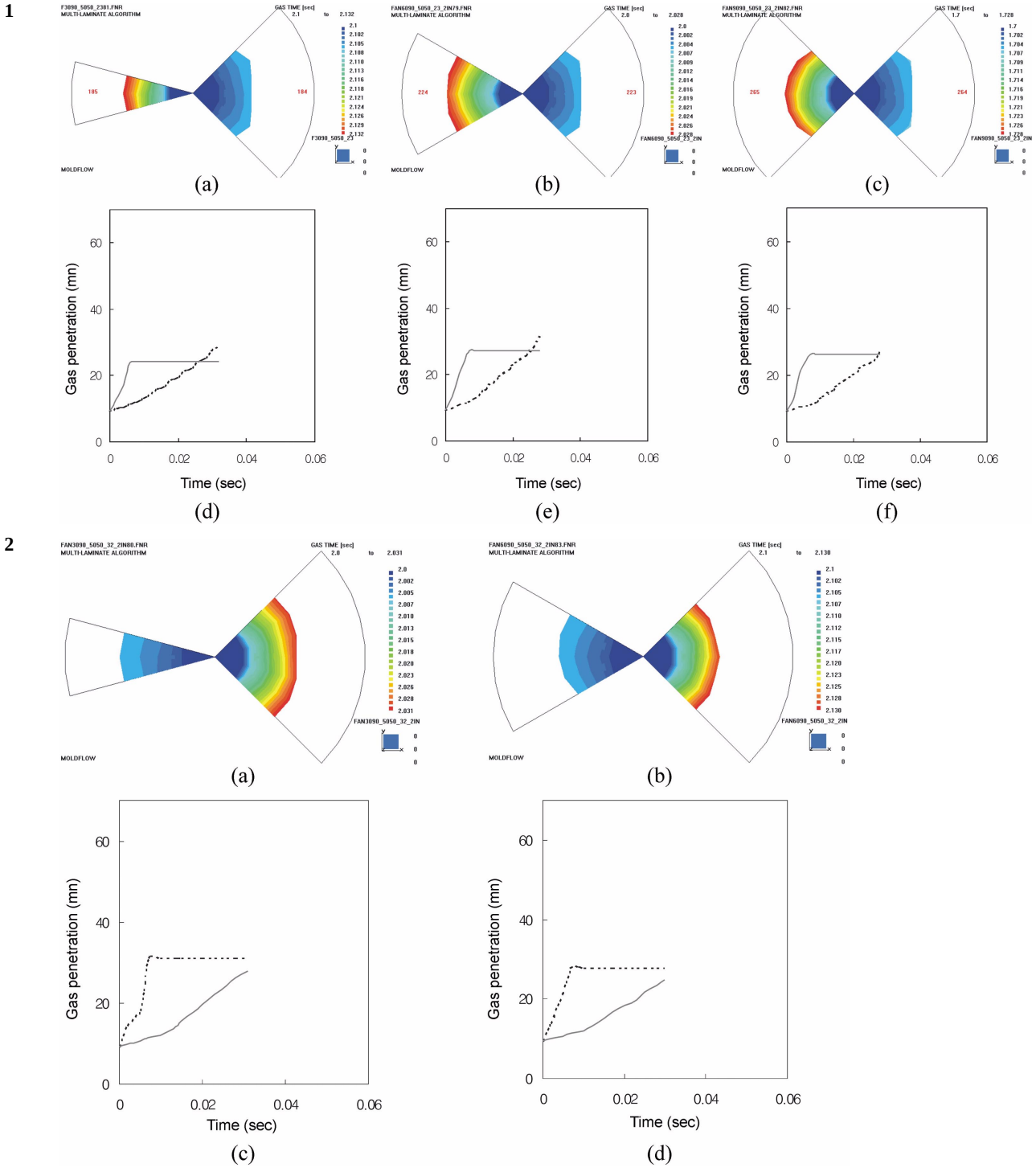

Fig. 3. 1(a) to 1(c) Simulated gas penetration (Refer to Table 2 for geometrical conditions.), 1(d) to 1(f) Gas penetration (Left: dotted line; Right: solid line): d) same condition as in 1(a); (e) same condition as in 1(b); (f) same condition as in 1(c). 2(a) to 2(b) Simulated gas penetration (Refer to Table 2 for geometrical conditions.), 2(c) to 2(d) Gas penetration (Left: dotted line; Right: solid line): (c) same condition as in 2(a); (d) same condition as in 2(b). 3(a) to 3(c) Simulated gas penetration (Refer to Table 2 for geometrical conditions.), 3(d) to 3(f) Gas penetration (Left: dotted line; Right: solid line): d) same condition as in 3(a); (e) same as in 3(b); (f) same condition as in 3(c), 3(g) to 3(i) Model-predicted gas penetration (Left: dotted line; Right: solid line): g) same condition as in 3(a); (h) same condition as in 3(b); (i) same condition as in 3(c).

tively, when gas was injected into the cavity of molds.

Subsequently, each set of a simulation and its corresponding model-prediction was compared and was evaluated to estimate the accuracy of the model prediction and to predict the gas direction, which may be defined as that of longer length of gas penetration into between the right and left fan-shaped cavities when either of the right

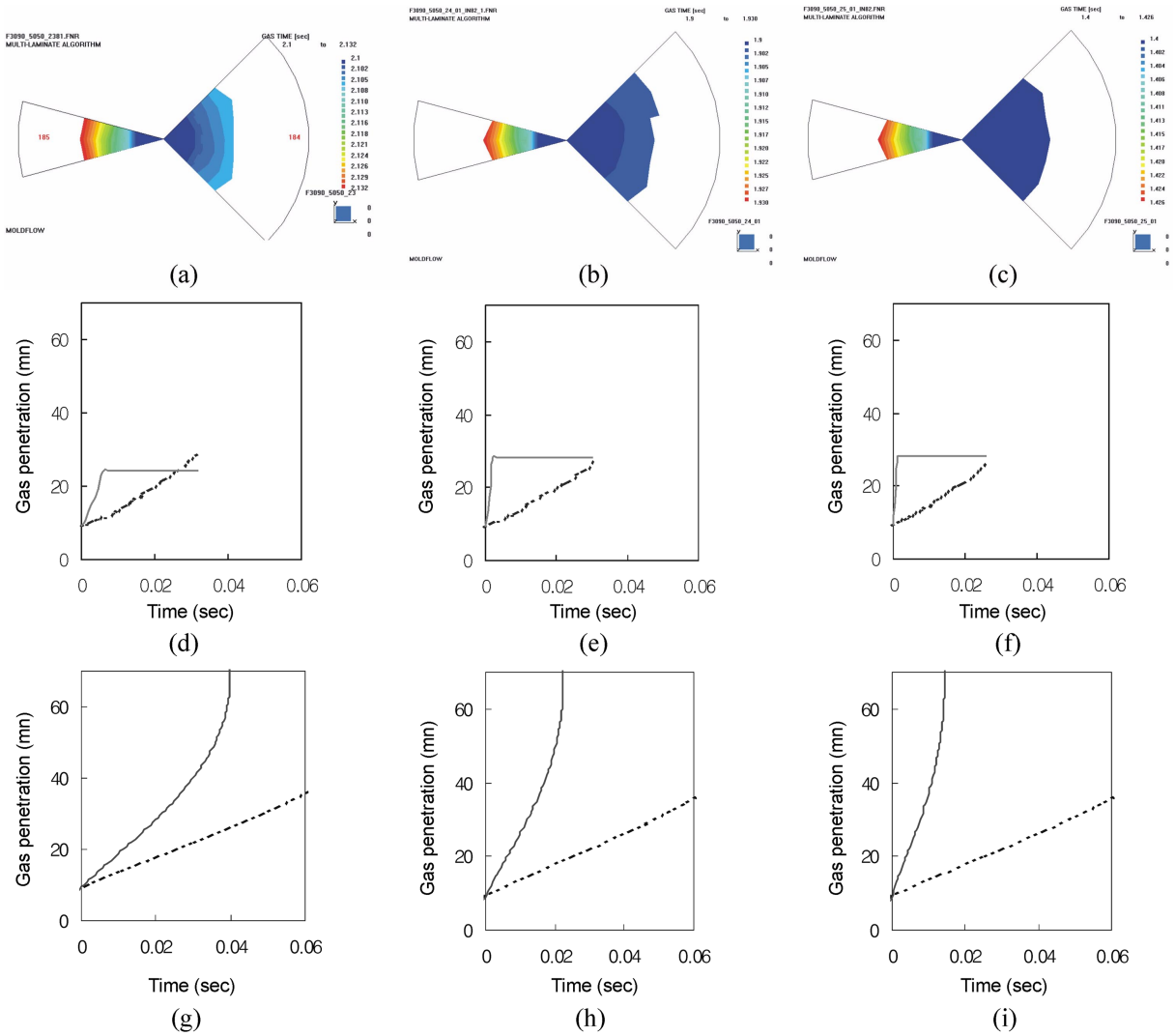

Fig. 3. Continued.

Table 3. Accuracy of model-predictions compared to the simulation-results in GAIM (1)

Simulation	Model-predictions	Ratio of H/R_0 (right/left)	SR	MR	Accuracy
Fig. 3-3(d)	Fig. 3-3(g)	1.49	4.4	2.98	Excellent
Fig. 3-3(e)	Fig. 3-3(h)	1.98	17.5	6.9	Good
Fig. 3-3(f)	Fig. 3-3(i)	2.55	32.0	10.0	Good

• SR denotes the ratio of simulated gas penetration lengths (right/left) to both of right and left directions when either of right and left leading fronts of melt polymer reaches mold barrier first.
• MR denotes the ratio of model-predicted gas penetration lengths (right/left) to both of right and left directions when either of right and left leading fronts of melt polymer reaches the maximum-distance first.
• Accuracy describes the degree of consistency between simulation results and model-predictions according to:
1) $|SR-MR|/SR<0.5$: Excellent
2) $0.5<|SR-MR|/SR<1$: Good
3) $1<|SR-MR|/SR<3$: Fair
4) $|SR-MR|/SR>3$: Bad:

and left leading melt-polymer fronts reaches the mold barrier first.

RESULTS AND DISCUSSION

1. Effective Solution of the Novel Flow Model

Differentiating both sides of Eq. (9) one may find the value of $R_1(t)$ that makes the inverse of dR_1/dt zero, in other words, makes the value of dR_1/dt infinite. Similarly, differentiating Eq. (9) with $R_1^2(t)$ one may obtain:

$$\Delta P\frac{dt}{dX}=\frac{3\mu}{(H-2\delta)^2}\ln\left[\left(\frac{2A}{\tilde{\theta}H}+R_1^2(0)\frac{2\delta}{H}\right)\frac{1}{X}+\left(1-\frac{2\delta}{H}\right)\right] \tag{11}$$

where $X=R_1^2(t)$

In order to make the value of dt/dX become zero, X may be chosen as:

$$X=\frac{H}{2\delta}\left(\frac{2A}{\tilde{\theta}H}+R_1^2(0)\frac{2\delta}{H}\right) \tag{12}$$

where $X=R_1^2(t)$

Substituting such value of $R_1^2(t)$ into Eq. (10), one may find the time

Table 4. Various geometrical conditions of fan-shaped cavities (2)

Case	Position	Vertex angle	Thickness	R_1	R_0
Fig. 4(a)	Left	30°	1 mm	3.1 mm	10 mm
	Right	30°	1.2 mm	4.8 mm	20 mm
Fig. 4(b)	Left	30°	1 mm	3.1 mm	10 mm
	Right	30°	1.5 mm	4.8 mm	20 mm
Fig. 4(c)	Left	30°	1 mm	3.1 mm	10 mm
	Right	30°	2 mm	4.8 mm	20 mm
Fig. 5(a)	Left	30°	1 mm	1.4 mm	10 mm
	Right	30°	1.1 mm	4.8 mm	40 mm
Fig. 5(b)	Left	30°	1 mm	1.4 mm	10 mm
	Right	30°	1.2 mm	4.8 mm	40 mm
Fig. 5(c)	Left	30°	1 mm	1.4 mm	10 mm
	Right	30°	2 mm	4.8 mm	40 mm
Fig. 5(d)	Left	30°	1 mm	1.4 mm	10 mm
	Right	30°	3 mm	4.8 mm	40 mm

when the melt front resin pushed forward would be used up due to coating the surface of molds. Since the coated layer left behind was considered in such a model-prediction that melt resin flow of declining mass due to accumulated coated layer may accelerate the gas flow, the trajectory of $R_1(t)$, i.e., gas penetration, showed an infinite value of its gradient with time, as in Fig. 2(d), when melt front resin pushed forward was used up to coat the surface of molds. The solution of Eq. (10) is valid in the part of time-dependent trajectory of $R_1(t)$ lower than $R_1(t)$ that makes the value of dR_1/dt infinite. Thus, the effective gas penetration of every figure in the model-predictions of Tables 3, 5 and 7 is the lower part from two parts of time-dependent trajectory in symmetry. However, the proposed model is not capable of showing the constant length of gas penetration after the leading front of melt polymer reaches mold barriers.

2. Results with Different Angle of Fans and Different Thickness of Fan-shaped Cavity

The commercial software Moldflow (version of MPI 4.0) was

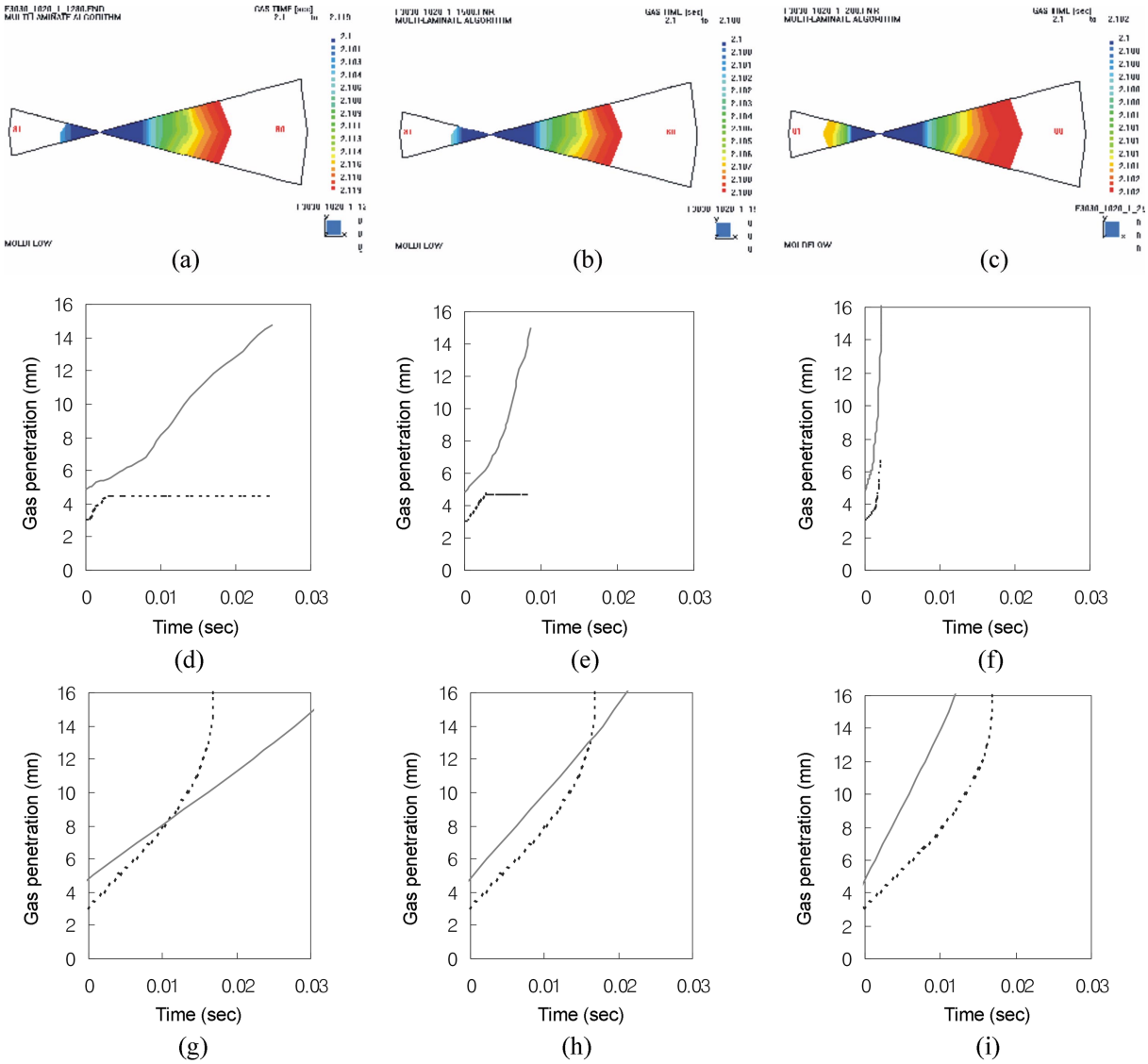

Fig. 4. (a) to (c) Simulated gas penetration (Refer to Table 4 for geometrical conditions.), (d) to (f) Gas penetration (Left: dotted line; Right: solid line): d) same condition as in (a); (e) same condition as in (b); (f) same condition as in (c), (g) to (i) Model-predicted gas penetration (Left: dotted line; Right: solid line): g) same condition as in (a); (h) same condition as in (b); (i) same condition as in (c).

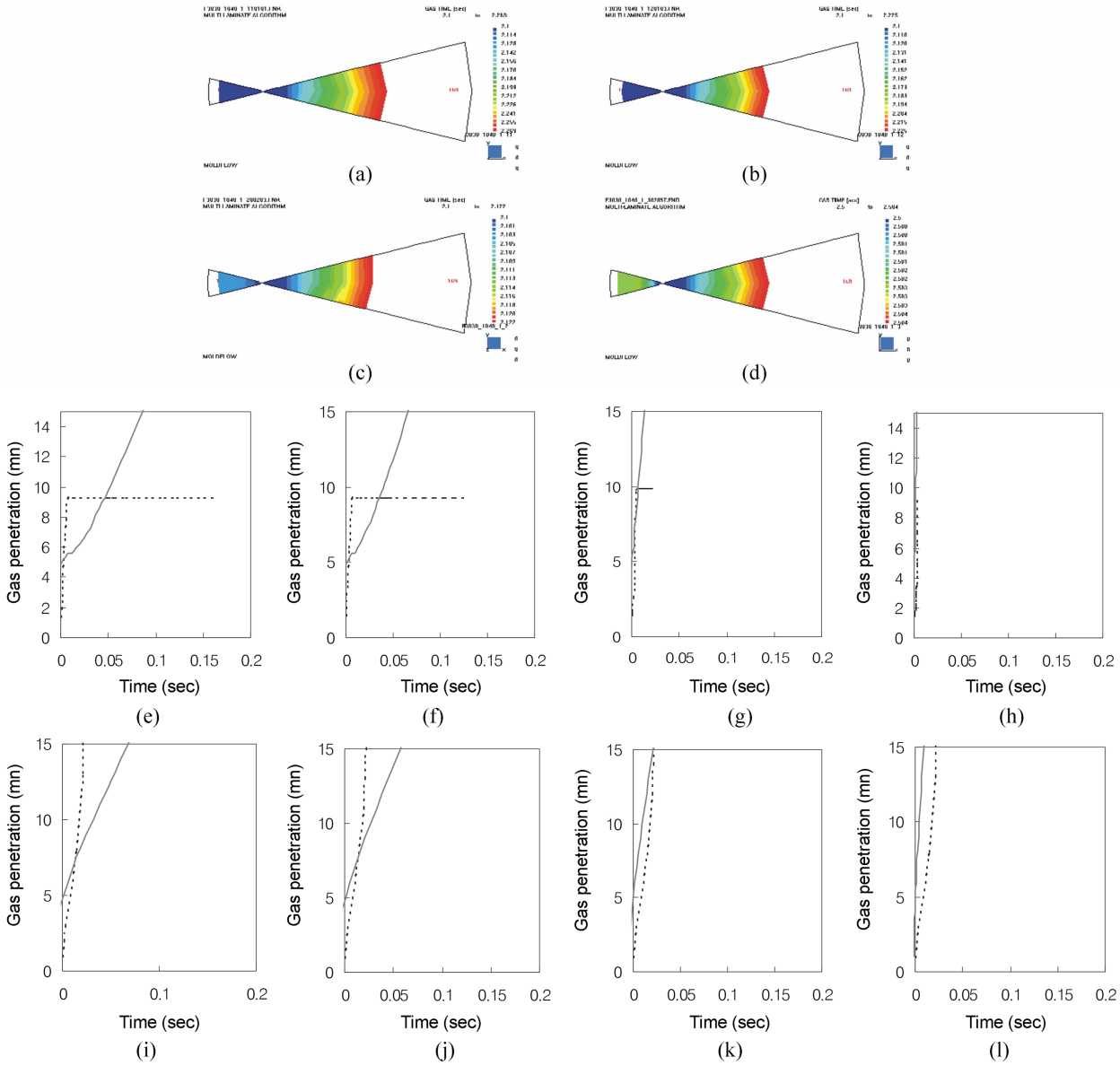

Fig. 5. (a) to (d) Simulated gas penetration (Refer to Table 4 for geometrical conditions.), (e) to (h) Gas penetration (Left: dotted line; Right: solid line): (e) same condition as in (a); (f) same condition as in (b); (g) same condition as in (c); (h) same condition as in (d), (i) to (l) Model-predicted gas penetration (Left: dotted line; Right: solid line): i) same condition as in (a); (j) same condition as in (b); (k) same condition as in (c); (l) same condition as in (d).

used to perform the simulations, of which conditions are given as in Table 1. Table 3 shows the accuracy of model-predictions compared to the simulation-results with various geometrical conditions as in Table 2. The simulation results of Figs. 3-1(a) to 3-1(c), 3-2(a) to 3-2(b), and 3-3(a) to 3-3(c) were transformed into Figs. 3-1(d) to 3-1(f), 3-2(c) to 3-2(d), and 3-3(d) to 3-3(f), respectively, that show the time-dependent trajectory of both directions of gas flows. Besides Figs. 3-3(g) to 3-3(i) deal with the results of model prediction corresponding to Figs. 3-3(d) to 3-3(f), respectively, and show their time-dependent model-based trajectory of both directions of gas flows.

It was noted that the simulation results were consistent with the model predictions in that the dynamic behavior of the interface between gas and melt resin was independent of the magnitude of a vertex angle of fan-shaped mold near a gas nozzle, as in Figs. 3-1(a) to 3-1(c) as well as Figs. 3-2(a) to 3-2(b).

In such transformed simulation-results as in Figs. 3-1(d) to 3-1(f), 3-2(c) to 3-2(d) and 3-3(d) to 3-3(f), gas penetration lengths, i.e., the distances traveled of the interface between gas-phase and melt polymer to both of right and left directions, were simulated until either of the leading fronts of melt polymer reached mold barrier first. Once either leading melt front reached the mold barrier, its time-dependent trajectory became flat afterwards. It was observed that at the side where resin ran faster the resin flow was blocked after the resin reached the barrier of molds, and the flow direction was reversed to the other direction.

In particular, it was remarkable that model-predictions described time-dependent behavior to both directions so accurately compared

Table 5. Accuracy of model-predictions compared to the simulation-results in GAIM (2)

Simulation	Model-predictions	Ratio of H/R_0 (left/right)	SR	MR	Accuracy
Fig. 4(d)	Fig. 4(g)	1.67	0.50	0.42	Excellent
Fig. 4(e)	Fig. 4(h)	1.33	0.85	0.67	Excellent
Fig. 4(f)	Fig. 4(i)	1	1.83	1.13	Excellent
Fig. 5(e)	Fig. 5(i)	3.57	0.08	0.35	Bad
Fig. 5(f)	Fig. 5(j)	3.33	0.08	0.36	Bad
Fig. 5(g)	Fig. 5(k)	2	0.35	0.25	Fair
Fig. 5(h)	Fig. 5(l)	1.33	1.38	1.5	Excellent

• SR denotes the ratio of simulated gas penetration length (right/left) to both of right and left directions when either of right and left leading fronts of melt polymer reaches mold barrier first.
• MR denotes the ratio of model-predicted gas penetration lengths (right/left) to both of right and left directions when either of right and left leading fronts of melt polymer reaches the maximum-distance first.
• Accuracy describes the degree of consistency between simulation results and model-predictions according to the same criteria applied as in Table 3.

to the results of simulation that both their predicted gas penetration length and their corresponding time scales were exactly matched to those by the simulation. However, the greater their ratios of thickness between right and left fans were, the greater SRs in the simulations became than MRs (that their model predicts) did, as shown in Table 3. This may be attributed to the fact that the shear rate thinning property of pseudo-plastic fluid made the velocity of gas flow faster than that from Eq. (10). Since the accuracies were generally above "Good" as in Table 3, the suggested gas-flow model may replace the simulations performed by commercial software within the given operating conditions of GAIM.

3. Results with Different Lengths of Initial Polymer Shut-off and Different Thickness of Cavities

The commercial software Moldflow (version of MPI 4.0) was again used to perform simulations, of which conditions are given as in Table 1. Table 5 shows the accuracy of model-predictions compared to the simulation results with various geometrical conditions as in Table 4. Figs. 4(a) to 4(c) and Figs. 5(a) to 5(d) were transformed into Figs. 4(d) to 4(f) and Figs. 5(e) to 5(h), respectively, which show the time-dependent trajectory of both directions of gas flows. In addition, Figs. 4(g) to 4(i) and Figs. 5(i) and 5(l) deal with the results of model prediction corresponding to Figs. 4(d) to 4(f) and Figs. 5(e) and 5(h), respectively, and show their time-dependent model-based trajectory of both directions of gas flows.

It was remarkable that model-predictions described time-dependent behavior to both directions so accurately compared to the results of simulation that their predicted gas penetration length and their corresponding time scale of Figs. 4(g) to 4(i) were rationally matched to those by the simulation in Figs. 4(d) to 4(f). However, just like the previous cases, the discrepancy between SR and MR was observed to increase between in Figs. 5(e) to 5(h) and in Figs. 5(i) to 5(l), respectively, as the ratio of the values of H/R_0 became bigger. This may also be attributed to the fact that their edge effect

Table 6. Various geometrical conditions of fan-shaped cavities (3)

Case	Position	Vertex angle	Thickness	R_1	R_0
Fig. 6(a)	Left	60°	2 mm	9.4 mm	43 mm
	Right	60°	3 mm	9.4 mm	43 mm
Fig. 6(b)	Left	60°	3 mm	9.4 mm	43 mm
	Right	60°	2 mm	9.4 mm	43 mm
Fig. 6(c)	Left	60°	2 mm	9.4 mm	43 mm
	Right	60°	5 mm	9.4 mm	43 mm

Table 7. Accuracy of model-predictions compared to the simulation-results in GAIM (3)

Simulation	Model-predictions	Ratio of H/R_0 (left/right)	SR	MR	Accuracy
Fig. 6(d)	Fig. 6(g)	3.57	0.26	0.28	Excellent
Fig. 6(e)	Fig. 6(h)	3.33	0.26	0.31	Excellent
Fig. 6(f)	Fig. 6(i)	2.00	0.52	0.76	Excellent

• SR denotes the ratio of simulated gas penetration lengths (right/left) to both of right and left directions when either of right and left leading fronts of melt polymer reaches mold barrier first.
• MR denotes the ratio of model-predicted gas penetration lengths (right/left) to both of right and left directions when either of right and left leading fronts of melt polymer reaches the maximum-distance first.
• Accuracy describes the degree of consistency between simulation results and model-predictions according to the same criteria applied as in Table 3.

was doubled than those in Figs. 4(a) to 4(c) due to doubled R_0 as in Figs. 5(a) and 5(d). As far as the gas direction is concerned, when the direction of gas flow is defined as that of longer length of gas penetration between through right and left fan-shaped cavities until either of the right and left leading melt-polymer fronts reaches the mold barrier first, it was always correct even though the accuracy was "Bad" in the cases of relatively small vertex angle (i.e., $\pi/6$) of a fan-shaped mold as well as relatively large value of the ratio of H/R_0.

With various geometrical conditions as in Table 6, Table 7 shows the accuracy of model-predictions compared to the results of simulation on the direction of gas flow of GAIM. Figs. 6(a) to 6(c) describe the simulation results of each process conditions and were transformed into Figs. 6(d) to 6(f) that show the time-dependent trajectory of both directions of gas flows. Figs. 6(g) to 6(i) deal with the results of model prediction corresponding to Figs. 6(d) to 6(f), respectively, and show their time-dependent model-based trajectory of both directions of gas flows.

The values of MR from Figs. 6(g) and 6(i) approached very closely to those of SR from Figs. 6(d) to 6(f), respectively, even though the ratios of H/R_0 were not small compared to those of Figs. 5(e) to 5(h). Thus, it was confirmed that the edge effect was quite diminished in cases of Figs. 6(a) to 6(c), where the vertex angle of fan-shaped molds was $\pi/3$, that their accuracy belonged to "Excellent" while the accuracies of Figs. 5(a) to 5(d), where their vertex angles were $\pi/6$, remained around " Fair". Since the accuracies of model predictions of Figs. 6(g) to 6(i) were "Excellent" as shown in Table

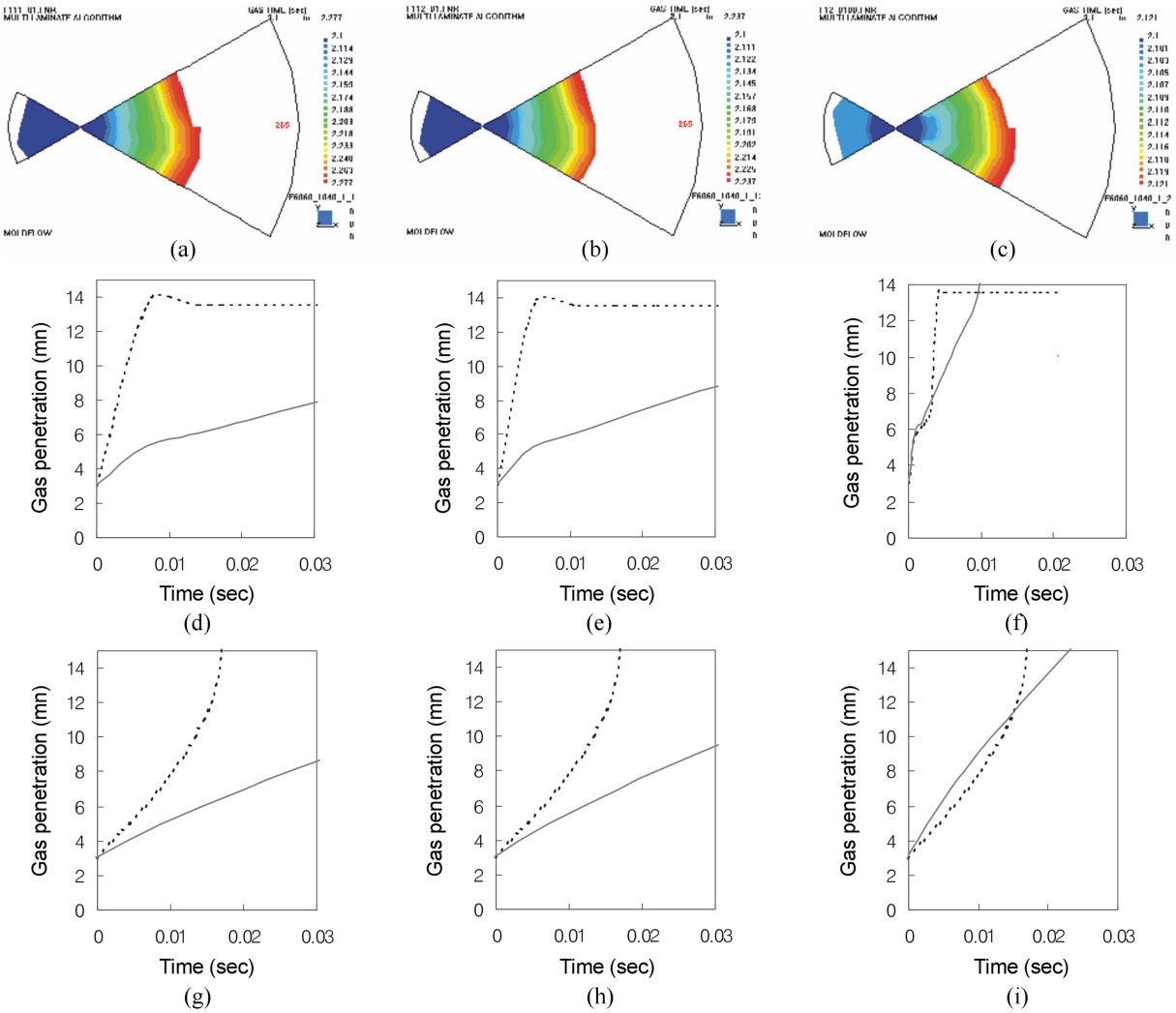

Fig. 6. (a) to (c) Simulated gas penetration (Refer to Table 6 for geometrical conditions.), (d) to (f) Gas penetration (Left: dotted line; Right: solid line): d) same condition as in (a); (e) same condition as in (b); (f) same condition as in (c), (g) to (i) Model-predicted gas penetration (Left: dotted line; Right: solid line): g) same condition as in (a); (h) same condition as in (b); (i) same condition as in (c).

7, the suggested gas-flow model may replace the simulations performed by commercial software within the given operating conditions of GAIM.

CONCLUSIONS

In GAIM a time-dependent-flow model was suggested under fan-shaped geometry in consideration of a coated layer on the surface of molds. The coated layer thickness has been well known to be associated with the capillary number (Ca). At the typical working range of GAIM (i.e., Ca>1,000), the hydrodynamic layer left behind occupies a certain number of fractions of the melt resin. In addition to hydrodynamic layer, the frozen layer at the surface of molds should also be considered to figure out the amount of resin left behind in GAIM. According to the results of simulations using MOLDFLOW (version of MPI 4.0), the polymer fraction turned out to be around 40% on the surface of fan-shaped cavities. Consequently, time evolutions of gas penetration lengths were predicted according to the model suggested assuming the thickness (δ) of each coated layer on each plate of fan-shaped molds to be 20% of thickness of the cavity. In model-predictions, the valid trajectory of $R_1(t)$ was the lower part between two parts of time-dependent trajectory in symmetry.

When different vertex angle of fans, different thickness of fan-shaped cavity and the same lengths of polymer shut-off on both sides were applied as geometrical conditions of fan-shaped molds, the model-predicted accuracies were generally above "Good," as in Table 3, even though melt-PET, which is reported to be a non-Newtonian fluid, was treated as a Newtonian fluid so that the suggested gas-flow model may replace the simulations performed by commercial software within the given operating conditions of GAIM. On the other hand, different lengths of initial polymer shut-off, different thickness of cavities and the same vertex angles of fans on both sides were used as the geometrical conditions. In those cases the discrepancy between SR and MR was observed, as in Table 5, to increase as the ratio of the values of H/R_0 on left and right sides became bigger. This may also be attributed to the fact that their edge effect was unbalanced on both sides due to their different lengths

of initial polymer shut-offs. As far as the gas direction was concerned, it was always correct even though the accuracy was "Bad" in the cases of relatively small angle (i.e., $\pi/6$) of a fan-shaped mold as well as relatively large value of the ratio of H/R_0, as in Table 5.

However, the model predicted trajectorys accuracy of the additional cases from Table 6 with the same geometrical conditions as in the previous cases from Table 4 except for wider vertex angles (i.e., $\pi/3$) of two fan-shaped molds, turned out to be "Excellent" as in Table 7. Since the accuracies were generally around "Excellent," the suggested gas-flow model may replace the simulations performed by commercial software within the given operating conditions of GAIM.

ACKNOWLEDGMENT

This research was supported (in part) by the Daegu University Research Grant, 2002.

NOMENCLATURE

A : injected volume of melt resin into fan-shaped geometry for initial polymer shut-off
h : distance between top or bottom plate and centerline of the cavity
H : distance between two parallel plates
MR : ratio of model-predicted gas penetration lengths (right/left) to both of right and left directions when either of right and left leading fronts of melt polymer reaches the maximum-distance first
P : pressure
P_1 : pressure at $r=R_1$
P_0 : pressure at $r=R_0$
Q : flow rate of melt resin
r : radial coordinate
R_1 : radius of nozzle for melt-resin/gas injection
R_0 : radius of initial polymer shut off
SR : ratio of simulated (by MOLDFLOW) gas penetration lengths (right/left) to both of right and left directions when either of right and left leading fronts of melt polymer reaches mold barrier first
t : time
V_r : velocity in r direction
V_1 : velocity in r direction at $r=R_1$
$\langle V_r \rangle$: average radial velocity

Greek Letters

δ : coated layer thickness
$\tilde{\theta}$: angle of the fan-shaped radial flow
μ : Newtonian viscosity

REFERENCES

Chen, S.-C., Cheng, N.-T. and Hsu, K.-S., "Simulations and Verification of the Secondary Gas Penetration in a Gas Assisted Injection Molded Spiral Tube," *International Communications in Heat and Mass Transfer*, **22**, 319 (1995)

Chen, S.-C., Cheng, N.-T. and Hsu, K.-S., "Simulations of Gas Penetration in Thin Plates Designed with a Semicircular Gas Channel During Gas Assisted Injection Molding," *Int. J. Mech. Sci.*, **38**, 335 (1996a).

Chen, S.-C., Cheng, Hsu, K.-F. and Hsu, K.-S., "Polymer Melt Flow and Gas Penetration in Gas Assisted Molding of a Thin Part with Gas Channel Design," *Int. J. Heat Mass Transfer*, **39**, 2957 (1996b).

Chen, S.-C., Cheng, N.-T. and Chao, S.-M., "Simulations and Verification of Melt Flow and Secondary Gas Penetration During a Gas Assisted Injection Molding," *International Polymer Processing*, **14**, 90 (1998).

Gao, D. M., Nguyen, K. T., Garcia-Rejon, and Salloum, G., "Optimization of the Gas Assisted Injection Moulding Process Using Multiple Gas-injection Systems," *Journal of Materials Processing Technology*, **69**, 282 (1997).

Gauri, V. G. and Koelling, K. W., "Gas-assisted Displacement of Viscoelastic Fluids: Flow Dynamics at the Bubble Front," *J. Non-Newtonian Fluid Mech.*, **83**, 183 (1999).

Huzyak, P. C. and Koelling, K. W., "The Penetration of a Long Bubble through a Viscoelastic Fluid in a Tube," *J. Non-Newtonian Fluid Mech.*, **71**, 73 (1997).

Khayat, R. E., Derdouri, A. and Herbert, L. P., "A Three-dimensional Boundary-element Approach to Gas Assisted Injection Molding," *J. Non-Newtonian Fluid Mech.*, **57**, 253 (1995).

Kolb, W. B. and Cerro, R. L., "Coating the Inside of a Capillary of Square Cross Section," *Chem. Eng. Sci.*, **46**(9), 2181 (1991).

Lim, K. H. and Lee, E. J., "Prediction of Gas Flow Directions in Gas Assisted Injection Molding When Cavities and Runners are Involved," *Korean J. Chem. Eng.*, **20**, 592 (2003).

Lim, K. H. and Soh, Y. S., "The Diagnosis of Flow Direction Under fan Shaped Geometry in Gas Assisted Injection Molding," *Journal of Injection Molding Technology*, **3**, 31 (1999).

Lim, K. H., "Flow Direction When Fan Shaped Geometry is Applied in Gas-Assisted Injection Molding: 1. Flow Model Theory and its Criteria for Predicting Flow Directions," *Korean J. Chem. Eng.*, **21**, 48 (2004).

McCabe, W. L., Smith, J. C. and Harriot, P., "Unit Operations of Chemical Engineering," 4th Ed., McGraw-Hill Press (1986).

Parez, M. A., Ong, N. S., Lam, Y. C. and Tor, S. B., "Gas-assisted Injection Molding: the Effects of Process Variables and Gas Channel Geometry," *Journal of Material processing Technology*, **121**, 27 (2002).

Poslinski, A. J., Oehler, P. R. and Stokes, V. K., "Isothermal Gas-assisted Displacement of vIscoplastic Liquids in Tubes," *Polym. Eng. Sci.*, **35**, 877 (1995).

Shen, Y. K., "Study on the Gas-liquid Interface and Polymer Melt Front in Gas Assisted Injection Molding," *Int. Comm. Heat Mass Transfer*, **24**, 295 (1997).

Shen, Y. K., "Study on Polymer Melt Front, Gas Front and Solid Layer in Filling Stage of Gas Assisted Injection Molding," *Int. Comm. Heat Mass Transfer*, **28**, 139 (2001).

Soh, Y. S. and Lim, K. H., "Control of Gas Direction in Gas Assisted Injection Molding; Definition of Resistance to Velocity, $r_{\bar{v}}$," SPE ANTEC Tec. Papers, **60**, 482 (2002).